

Insights into water coordination associated to the Cu^{II}/aCu^I electron transfer at a biomimetic Cu centre

Ana Gabriela Porras Gutiérrez,^a Joceline Zeitouny,^a Antoine Gomila,^a Bénédicte Douziech,^a Nathalie Cosquer,^a Françoise Conan,^a Olivia Reinaud,^b Philippe Hapiot,^c Yves Le Mest,^a Corinne Lagrost,^{*c} and Nicolas Le Poul^{*a}

Abstract

The coordination properties of the biomimetic complex [Cu(TMPA)(H₂O)](CF₃SO₃)₂ (TMPA=tris(2-pyridylmethyl)amine) have been investigated by electrochemistry combined to UV-Vis and EPR spectroscopies in different non-coordinating media including imidazolium-based room-temperature ionic liquids, for different water contents. The solid-state X-ray diffraction analysis of the complex shows that the cupric centre lies in a N₄O coordination environment with a nearly perfect trigonal bipyramidal geometry (TBP), the water ligand being axially coordinated to Cu^{II}. In solution, the coordination geometry of the complex remains TBP in all media. Neither the triflate ion nor the anions of the ionic liquids were found to coordinate the copper centre. Cyclic voltammetry in all media shows that the decoordination of the water molecule occurs upon monoelectronic reduction of the Cu^{II} complex. Back-coordination of the water ligand at the cuprous state can be detected by increasing the water content and/or decreasing the timescale of the experiment. Numerical simulations of the voltammograms allow the determination of kinetics and thermodynamics for the water association-dissociation mechanism. The resulting data suggest that (i) the binding/unbinding of water at the Cu^I redox state is relatively slow and equilibrated in all media, and (ii) the binding of water at Cu^I is somewhat faster in the ionic liquids than in the non-coordinating solvents, while the decoordination process is weakly sensitive to the nature of the solvents. These results suggest that ionic liquids favour water exchange without interfering with the coordination sphere of the metal centre. This makes them promising media for studying host-guest reactions with biomimetic complexes.

Introduction

Reorganizational processes coupled to electron transfer are of particular importance in many chemical and biological systems associated to the Cu^{II}/Cu^I reaction.¹ Such processes are due to crystal field forces and Jahn-Teller effects when passing from Cu^I (d¹⁰) to Cu^{II} (d⁹). They involve most of the time the coordination/decoordination of one or several donor ligands together with geometric changes. The Cu^I (d¹⁰) ion is quite “plastic” toward its environment and can readily adopt 2-, 3- or 4-coordinated geometry. Contrariwise, the Cu^{II} (d⁹) ion has a strong preference for tetragonal environments, leading to 5- and 6-coordinated cores, and Cu^{II} can exert a strong electronic/geometric effect on its surroundings in the absence of sterical constraints. Many studies have been devoted to understand/control this chemical upheaval with the variation of the electronic/geometric/steric environment of the copper centre, using mainly synthetic Cu complexes as model systems.^{1a} One of the most popular system is the mononuclear complex [Cu^{II}(TMPA)(L)]²⁺ (L=solvent), based on the tripodal tetradentate ligand TMPA (TMPA = tris(2-pyridylmethyl)amine), which is a ligand of choice for mimicking metallo enzymes of relevance to oxygen activation, for instance. This complex and its derivatives have been studied in depth over the past years since they react at Cu^I redox state with dioxygen to form transient Cu_nO₂ reactive species.^{2,3,4} Recent works have shown that these derivatives were able to activate dioxygen, leading to the catalytic oxidation of organic substrates as homogeneous catalysts^{5,6,7}, or to reduce O₂ into H₂O by heterogeneous catalysis.⁸ Also, in acidic aqueous media, catalytic properties towards reduction of nitrite ions into nitric oxide were emphasized by voltammetric studies for [Cu^I(TMPA)(H₂O)]⁺.⁹ In another connection, Le Mestret *al.* have used the nitrilo Cu complex [Cu^{II}(TMPA)(CH₃CN)]²⁺ for evidencing secondary-sphere effects at the redox level by comparison with a more sophisticated complex.¹⁰

The chemical modifications associated to the electronic transfer are usually detected by complementing spectroscopic studies (NMR, EPR, UV-Vis...) with electrochemical techniques (often cyclic voltammetry). In almost all cases, the electrochemical studies of [Cu^{II}(TMPA)(L)]²⁺ were performed in coordinating solvents (DMF, CH₃CN, H₂O) and/or in presence of coordinating anion (Cl⁻, N₃⁻). The purpose of these studies was essentially to compare the donating effect of each ligand by correlation with the thermodynamic standard potential value E^0 in the same solvents, the redox potential being highly influenced by electronic, steric and geometric factors. So far, none of the voltammetric studies in solution have ever intended to investigate the chemical mechanisms associated to the Cu^{II/I} electron exchange. Particularly the water ligand(s) decoordination process at Cu^I redox state has not been explored by electrochemistry, despite its high interest. Indeed, water plays an important role in many enzymatic processes.¹¹ In particular, it was shown that water could inhibit oxygen reaction in cytochrome c oxidase models.¹² Also, it can affect the redox potential of proteins

through secondary sphere effects.¹³ Recently, water molecules in the active site of Cu-nitrite reductase, were shown to specifically protect from nitrite coordination at Cu(II) and favor catalytic activation at Cu(I) by displacement of the water ligand.¹⁴ Water dissociation is thus of fundamental importance in the activation process. Here we propose to explore such a phenomenon with water as an exogenous ligand with a TMPA Cu complex.

Herein, with the help of electrochemistry combined to EPR/UV-Vis spectroscopies, we report a detailed study of the behaviour of the $[\text{Cu}^{\text{II}}(\text{TMPA})(\text{H}_2\text{O})](\text{CF}_3\text{SO}_3)_2$ complex upon electron transfer in different non-coordinating media including dichloromethane (CH_2Cl_2), tetrahydrofuran (THF), propylene carbonate (PC) and imidazolium-based room temperature ionic liquids (RTILs) (Scheme 1). This study is aimed at investigating the chemical processes associated to the $\text{Cu}^{\text{II/I}}$ electron transfer reaction, particularly the possible release of the water molecule at the Cu^{I} redox state in terms of kinetics and thermodynamics. Ionic liquids are liquid at room temperature (or close to) and are composed entirely of ions. Generally consisting in a combination of bulky organic cations and weakly coordinating anions, they possess several typical properties such as ionic conductivity, wide electrochemical window, high viscosity, high polarity, high thermal stability, negligible vapour pressure and the ability to dissolve a large range of organic or inorganic compounds.¹⁵ A major advantage of the ionic liquids is the ease of change of the anion/cation combination, allowing the preparation of highly “tunable” media especially designed for a specific application. As such, they nowadays cover a wide range of applications including synthetic chemistry, catalysis, (bio) analytical sensors, and material science.^{15,16} They have been widely used as solvents in fundamental electrochemical reactions.¹⁷ However ionic liquids have been scarcely considered as solvents for analysing the electrochemical reactivity of coordination metal complexes.¹⁸ While they can represent advantageous alternative to conventional solvents due to their intrinsic properties, their specific nature may also influence the coordination properties of the complexes. Thus, some studies have explored the coordinating properties of the anion from the ionic liquids towards metallic cations (Cu^{2+} , Li^+).^{19,20} Nevertheless, the influence of the RTILs as secondary sphere on the coordination properties of metallic complexes associated to their redox properties has not been investigated so far.

Results and Discussion

Fig. 1.A) ORTEP representation of $[\text{Cu}^{\text{II}}(\text{TMPA})(\text{H}_2\text{O})](\text{CF}_3\text{SO}_3)_2$ (50 % probability ellipsoids shown). Hydrogen and both triflate anions are omitted for clarity. **B)** Schematic representation of the $[\text{Cu}^{\text{II}}(\text{TMPA})(\text{H}_2\text{O})]^{2+}$ complex.

Scheme 1. Representation of the RTILs used in this study.

Synthesis and structural properties of the $[\text{Cu}^{\text{II}}(\text{TMPA})(\text{H}_2\text{O})](\text{CF}_3\text{SO}_3)_2$ complex.

The synthesis of the bis-triflate Cu complex $[\text{Cu}^{\text{II}}(\text{TMPA})(\text{H}_2\text{O})](\text{CF}_3\text{SO}_3)_2$ was inspired by the procedure developed for the bis-perchlorato analogous complex $[\text{Cu}^{\text{II}}(\text{TMPA})(\text{H}_2\text{O})](\text{ClO}_4)_2$.⁹ Blue single crystals were obtained and analysed by X-ray diffraction. As shown in Fig. 1, the cupric centre lies in a N_4O coordination mode with a nearly perfect trigonal bipyramidal geometry (TBP) ($\tau = 0.95$),²¹ the O(7)-Cu-N(4) angle being almost linear (176.91°) (see Table 1). Clearly, none of both triflate anions (CF_3SO_3^-) is coordinated to the Cu centre as previously reported for the bis-perchlorato analogous complex.⁹ Cu-N distances in the trigonal plane are almost equal (2.06 \AA), and N-Cu-N angles are close to the ideal 120° value. In the axial part, Cu-N(4) and Cu-O(7) distances are shorter (2.01 \AA and 1.95 \AA respectively) depicting strong interaction of the amine and the water ligands with the metal ion. These structural features are similar to those found for the perchlorato derivative $[\text{Cu}(\text{TMPA})(\text{H}_2\text{O})](\text{ClO}_4)_2$ ($\tau = 0.96$),⁹ emphasizing the minor role of the counter anions on the structural properties at the solid state.

Table 1 Selected bond distances and angles for [Cu^{II}(TPMA)(H₂O)](CF₃SO₃)₂. See Supporting Information part for details

	Distance /Å		Angle /°
Cu-N(1)	2.060(3)	O(7)-Cu-N(1)	98.5(1)
Cu-N(2)	2.058(3)	O(7)-Cu-N(2)	94.8(1)
Cu-N(3)	2.069(3)	O(7)-Cu-N(3)	99.9(1)
Cu-N(4)	2.011(3)	O(7)-Cu-N(4)	176.9(1)
Cu-O(7)	1.945(8)	N(1)-Cu-N(2)	119.9(1)
		N(1)-Cu-N(3)	117.3(1)
		N(1)-Cu-N(4)	82.4(1)
		N(2)-Cu-N(3)	117.4(1)
		N(2)-Cu-N(4)	82.2(1)
		N(3)-Cu-N(4)	82.2(1)

Table 2 EPR data (150 K) and UV-Vis data for [Cu^{II}(TPMA)(H₂O)](SO₃CF₃) in the different media.

Medium	[H ₂ O] /ppm	$g_{//}$ ($A_{//}/10^{-4}$ cm ⁻¹)	g_{\perp} ($A_{\perp}/10^{-4}$ cm ⁻¹)	λ_{\max} /nm (ϵ /M ⁻¹ cm ⁻¹) [‡]	λ_{\max} /nm (ϵ /M ⁻¹ cm ⁻¹) [#]
CH ₂ Cl ₂ dry	200 ^[a]	1.99 (66)	2.21 (103)	695 (54)	940 (249)
CH ₂ Cl ₂ wet	1900 ^[b]	2.00 (66)	2.21 (105)	694 (53)	898 (317)
THF dry	50 ^[c]	2.00 (64)	2.20 (106)	677 (67)	892 (185)
THF wet	1900 ^[d]	2.00 (64)	2.20 (106)	667 (120)	846 (215)
PC dry	150 ^[e]	2.00 (63)	2.20 (106)	689 (69)	895 (183)
PC wet	6800 ^[f]	2.00 (68)	2.20 (105)	682 (80)	870 (210)
[BMIm][NTf ₂] dry	50 ^[g]	1.99 (62)	2.20 (103)	676 (52)	892 (120)
[BMIm][NTf ₂] wet	3600 ^[h]	[i]	[i]	675 (64)	880 (175)
[BMIm][PF ₆] dry	77.5 ^[i]	[k]	[k]	[i]	[i]
[Et ₃ BuN][NTf ₂]	[i]	2.00	2.20 (105)	[i]	[i]
Solid state	[i]	[i]	[i]	647	826

Corresponding concentration in mol L⁻¹: ^[a] 1.5 10⁻², ^[b] 1.4 10⁻¹, ^[c] 2.5 10⁻³, ^[d] 9.5 10⁻², ^[e] 9.9 10⁻³, ^[f] 4.5 10⁻¹, ^[g] 4 10⁻³, ^[h] 2.9 10⁻¹, ^[i] 5.8 10⁻³. [i] not determined.

^[k] pseudo-axial spectrum $g_x = 2.21$ (117), $g_y = 2.17$ (117); $g_z = 1.99$ (72). [‡] $d_{xz,yz} \rightarrow d_{z^2}$ transition; [#] $d_{x^2-y^2,xy} \rightarrow d_{z^2}$ transition.

Spectroscopic studies in solution.

The coordination properties of [Cu(TPMA)(H₂O)](CF₃SO₃)₂ were examined by Electron Paramagnetic Resonance (EPR) and UV-Visible spectroscopies in three non-coordinating solvents (CH₂Cl₂, THF and PC) and in three different ionic liquids where both anions and cations were varied ([BMIm][NTf₂], [BMIm][PF₆] and [Et₃BuN][NTf₂]) (Scheme 1). Addition of coordinating species such as H₂O and CH₃CN was performed at room temperature for a full characterization of the coordinating environment around Cu^{II}, with a particular focus on the nature of the fifth exogenous ligand. Whatever the non-coordinating media, [Cu^{II}(TPMA)(H₂O)]²⁺ displays an EPR reversed axial spectral pattern with $g_{\perp} > g_{//} \approx 2.0$ (Fig. 2A and SI). The hyperfine coupling constants A_{\perp} have small values in the range 100-120 G (Table 2). These features are typical of a Cu^{II} complex in a TBP geometry with a d_{z^2} ground state, as previously observed for the nitrilo analogue [Cu^{II}(TPMA)(CH₃CN)]²⁺ in frozen acetonitrile. The g and A values are slightly different than those obtained in acetonitrile ($g_{\perp} = 2.19$, $g_{//} = 2.02$, $A_{\perp} = 113$ 10⁻⁴ cm⁻¹). Moreover, the addition of water at room temperature did not induce any modification of the frozen solution spectra (see SI for each solvent). Hence, taking into account that the EPR data are not affected at all by the presence of water whatever the solvent and that the donor ability of THF is much weaker compared to water, it can reasonably be concluded that H₂O is the fifth ligand in axial position in THF as well as in CH₂Cl₂ and PC, and that the solid state aqua TBP structure determined by XRD is kept in solution. The same conclusion could be drawn for the ionic liquids, as the EPR responses of the complex were almost identical to those obtained in CH₂Cl₂, THF and PC (Fig. 2A). Moreover, for the three different ionic liquids media, the recorded spectra were very

similar, evidencing that neither the nature of the cation (imidazolium vs ammonium) nor that of the anion (NTf_2^- vs PF_6^-) do modify the coordination properties of the $\text{Cu}^{\text{II}}\text{TMPA}$ complex in the ionic liquids. In the case of the anions, this result deserves to be emphasized because previous studies showed that the NTf_2^- anion, despite its non-coordinating nature, is able to bind ligand-deficient metal complexes through various nitrogen and/or oxygen binding modes.²² As for non-coordinating solvents, addition of acetonitrile to the ionic liquids yielded a change of the EPR response, indicating the substitution of H_2O by CH_3CN in the Cu^{II} coordination sphere. UV-Vis absorption analysis is in good concordance with EPR results. In all media, d-d transition bands in the 850-950 nm wavelength range, with a shoulder at ca. 680 nm were observed. This is indicative of a large contribution of trigonal bipyramidal TBP geometry in solution, as confirmed by the solid state spectrum of the complex (Table 2).²³

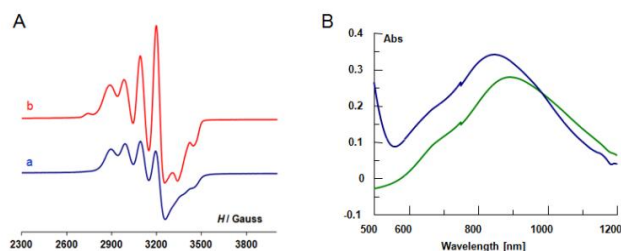


Fig. 2. A) EPR spectra at $T = 150$ K of $[\text{Cu}^{\text{II}}(\text{TMPA})(\text{H}_2\text{O})]^{2+}$ (10^{-3} mol L^{-1}) in a) “dry” CH_2Cl_2 ($[\text{H}_2\text{O}] = 1.5 \cdot 10^{-2}$ M (200 ppm)) and b) “dry” $[\text{BMIm}][\text{NTf}_2]$ ($[\text{H}_2\text{O}] = 4 \cdot 10^{-3}$ M (50 ppm)). B) UV-Vis spectra of $[\text{Cu}^{\text{II}}(\text{TMPA})(\text{H}_2\text{O})]^{2+}$ ($1.5 \cdot 10^{-3}$ mol L^{-1}) in dry (green) and wet (blue) THF.

Interestingly, the addition of water induces a significant shift of the λ_{max} value, between 10 and 50 nm in all media (see SI and Table 2). For instance, in THF, a shift of 46 nm is observed by addition of 1 % of water (Fig. 2B). This clearly shows, in agreement with EPR data, that it is not correlated to the coordination of the solvent. Possibly, this effect is due to the increased polarity of the solution and solvation of the counterion and/or water. To summarize, the spectroscopic solution studies show that H_2O remains coordinated to the cupric center in all the non-coordinating media starting from the solid-state characterized $[\text{Cu}^{\text{II}}(\text{TMPA})(\text{H}_2\text{O})]^{2+}$ complex. The geometric features of the Cu complex in solution are not significantly perturbed by the change of medium (TBP conformation) and water content. This point indicates that all voltammetric studies will be initiated with the same (geometry, coordination) complex $[\text{Cu}^{\text{II}}(\text{TMPA})(\text{H}_2\text{O})]^{2+}$ and is prerequisite for a comparison of the redox behavior and associated mechanisms in the different media.

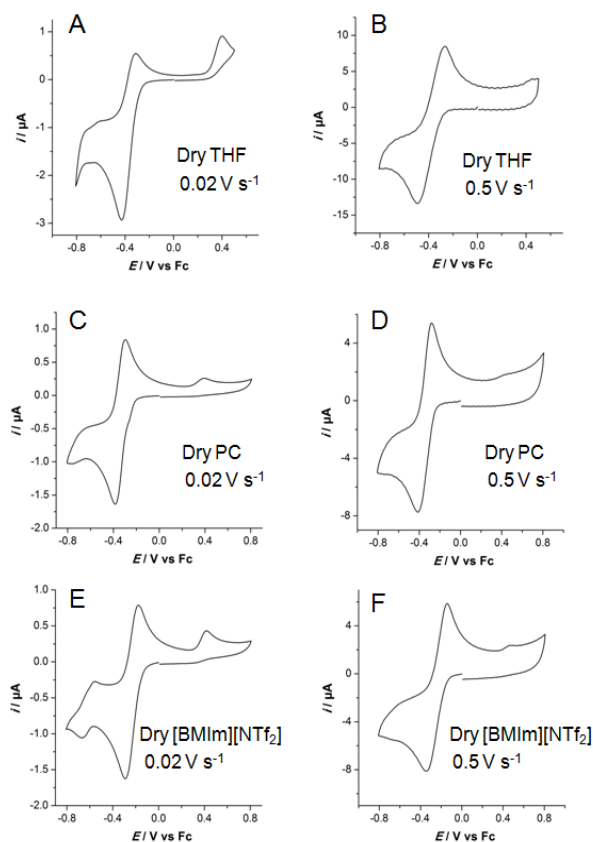


Fig. 3. Cyclic voltammetry of $[\text{Cu}^{\text{II}}(\text{TMPA})(\text{H}_2\text{O})]^{2+}$ ($\sim 10^{-3}$ mol L^{-1}) at a glassy carbon disk electrode at 0.02 V s^{-1} (left) and 0.5 V s^{-1} (right) in (A, B) “dry” THF ($[\text{H}_2\text{O}] = 2.5 \cdot 10^{-3}$ mol L^{-1}), (C, D) “dry” PC ($[\text{H}_2\text{O}] = 9.9 \cdot 10^{-3}$ mol L^{-1}) and (E, F) “dry” $[\text{BMIm}][\text{NTf}_2]$ ($[\text{H}_2\text{O}] = 4 \cdot 10^{-3}$ mol L^{-1}).

Table 3 Density (d), dynamic viscosity (η), static (ϵ_s) and optical (ϵ_{opt}) dielectric constant values for different media at $T = 20^\circ\text{C}$

Medium	$d / \text{g cm}^{-3}$	$\eta / \text{mPa s}$	ϵ_s	ϵ_{opt}^b
CH_2Cl_2	1.33	0.4	9.1	2.03
THF	0.89	0.5	7.6	1.98
PC	1.19	2.5	64.9	2.02
[BMIm][NTf ₂]	1.43	52	11.5 ^a	2.04
		40 (130 ppm H ₂ O)		
		33.8 (4180 ppm H ₂ O)		
[BMIm][PF ₆]	1.35	308	11.4	

[a] from ref. ²⁴ [b] Calculated from the square of the refractive index.²⁵

Electrochemical studies of the $[\text{Cu}^{\text{II}}(\text{TMPA})(\text{H}_2\text{O})]^{2+}$ complex.

Cyclic voltammetric experiments were performed in the different solvents containing NBu_4PF_6 as supporting salt, as well as in [BMIm][NTf₂] and in [BMIm][PF₆] as typical examples of ionic liquids. In addition to their non-coordinating nature, the solvents exhibit different properties of viscosity, polarity (Table 3) for allowing a comparative study of the influence of the medium on the redox behaviour of $[\text{Cu}^{\text{II}}(\text{TMPA})(\text{H}_2\text{O})]^{2+}$. The water content in the solvents was varied to examine the possible effect of the presence of water on the chemical processes associated to the electron transfer reaction for this aqua complex. For sake of clarity, solvents were

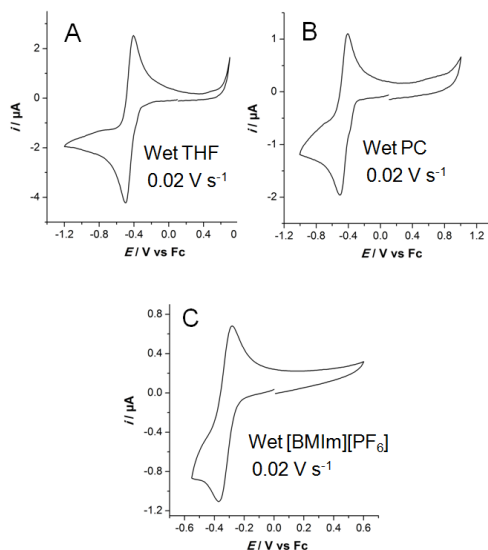


Fig. 4. Cyclic voltammetry of $[\text{Cu}^{\text{II}}(\text{TMPA})(\text{H}_2\text{O})]^{2+}$ ($\sim 3\text{--}5 \cdot 10^{-3} \text{ mol L}^{-1}$) at a glassy carbon disk electrode at $v = 0.02 \text{ V s}^{-1}$ in (A) “wet” THF ($[\text{H}_2\text{O}] = 9.5 \cdot 10^{-2} \text{ mol L}^{-1}$), (B) “wet” PC ($[\text{H}_2\text{O}] = 4.5 \cdot 10^{-1} \text{ mol L}^{-1}$) and (C) “wet” [BMIm][PF₆] ($[\text{H}_2\text{O}] = 1.9 \cdot 10^{-1} \text{ mol L}^{-1}$).

In THF, PC, [BMIm][NTf₂] and [BMIm][PF₆], cyclic voltammeteries display very similar patterns while the electrochemical behaviour in CH_2Cl_2 exhibits some slight differences (*vide infra*). For the four first media, a chemically reversible redox system located between $E_1^0 = -0.25$ and -0.4 V vs Fc is observed upon reduction at scan rates above 0.5 V s^{-1} . When decreasing the scan rates, the redox system appears less reversible ($i_{pa}/i_{pc} < 1$) whereas an additional irreversible oxidation peak becomes visible at more positive potential (*ca.* 0.4 V vs Fc) on the reverse scan (Fig.3). For ionic liquids media, an additional redox system of less intensity is also visible at -0.61 V and is due to the presence of residual chloride ions (from ionic liquids precursor), leading to the formation of a $[\text{Cu}^{\text{II}}\text{TMPA}(\text{Cl})]^+$ complex.[†] The amount of water in the media has a strong influence on the electrochemical behaviour of the copper complex. As the concentration of water is increasing, the anodic peak disappears while the redox system at E_1^0 tends to be more reversible, even at the lowest scan rates (Fig. 4). The electrochemical behaviour of $[\text{Cu}^{\text{II}}(\text{TMPA})(\text{H}_2\text{O})]^{2+}$ in CH_2Cl_2 is similar to those described above but it is complicated by a reaction between the cuprous complex, formed during the electrochemical reduction of the initial Cu^{II} complex, and dichloromethane to produce $[\text{Cu}^{\text{II}}(\text{TMPA})(\text{Cl})]^+$ as previously described by Karlin and co-workers.²⁶ A second reversible redox process could be then observed at -0.75 V , as in ionic liquids ($E^\circ = -0.61 \text{ V}$), except that it is not due, this time, to the presence of residual chloride ions (Fig. 5). Under mild conditions, the Cu^{I} complex reacts in a stoichiometric manner with alkyl or benzyls halides to produce near quantitative

yields of coupled products.²⁶ The copper center acts as the halogen atom abstractor and the halide Cu^{II} complex [Cu^{II}(TMPA)Cl]⁺ is formed. This chloro-Cu^{II} complex is then reversibly reduced at -0.75 V explaining the occurrence of the second reversible redox process in CH₂Cl₂. The formation of the chloro complex is fully corroborated by the addition of chloride to the solution, which leads to the formation of a reversible system at the same potential.

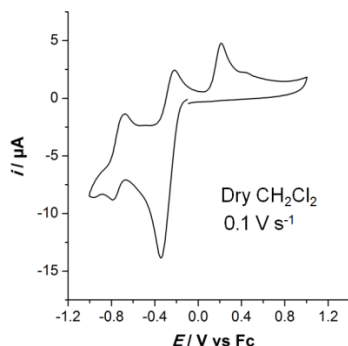


Fig. 5. Cyclic voltammetry of [Cu^{II}(TMPA)(H₂O)]²⁺ (~ 10⁻³ mol L⁻¹) at a glassy carbon disk electrode at $\nu = 0.1 \text{ V s}^{-1}$ in “dry” CH₂Cl₂.

Mass transport of [Cu^{II}(TMPA)(H₂O)]²⁺ complex.

For each medium, under dry conditions (Table 4), the diffusion coefficient (D) value for [Cu^{II}(TMPA)(H₂O)]²⁺ was estimated from current peak values by using the Randles-Sevcik equation.²⁷ The diffusion coefficient decreases as the viscosity of the medium is increasing, in agreement with the Stokes-Einstein relationship (1) :

$$D = \frac{k_B T}{6\pi\eta a_0} \quad (1)$$

where D is the diffusion coefficient, η is the dynamic viscosity of the medium, k_B is the Boltzmann constant, T is the absolute temperature, a_0 is the hydrodynamic radius of the species, and 6 is a numerical value being equal to 6 or 4 depending if the “stick” or the “slip” conditions apply. It can be noted that the Stokes-Einstein equation applies in ionic liquids in the case where the diffusing species are similar in size with the ions of the IL but was shown not to apply for small molecules such as dihydrogen or sulphur dioxide.²⁸ A non Stokesian behaviour has been even evidenced for concentrated iodide in ionic liquids.²⁹ In more recent works, Licence and co-workers have demonstrated that the Stokes-Einstein equation describes the behaviour of electroactive species such as ferrocenemethanol and ferrocenemethylimidazole in ionic liquids but the numerical value lies somewhere between 4 and 6.³⁰ As can also be observed, the [Cu^{II}(TMPA)(H₂O)]²⁺

Table 4 Selected electrochemical parameters for [Cu^{II}(TMPA)(H₂O)]²⁺ in the different media. E /V vs Fc

	“Dry” medium			“Wet” medium	
	10 ³ [H ₂ O]/ mol L ⁻¹	10 ⁶ D / cm ² s ⁻¹	E_1^0 /V	10 ³ [H ₂ O]/ mol L ⁻¹	E_1^0 /V
CH ₂ Cl ₂	15	6	-0.31	140	-0.33
THF	2.5	2.9	-0.38	94	-0.52
PC	9.9	0.58	-0.36	450	-0.48
[BMIm][NTf ₂]	4	0.06	-0.25	290	-0.38
[BMIm][PF ₆]	5.8	0.004	-0.22	200	-0.33

complex diffuses very slowly in the two ionic liquids, $D = 6 \cdot 10^{-12} \text{ m}^2 \text{ s}^{-1}$ in [BMIm][NTf₂] and $D = 0.4 \cdot 10^{-12} \text{ m}^2 \text{ s}^{-1}$ in [BMIm][PF₆]. For comparison, the diffusion coefficient of inorganic metal complexes such as ferrocene or ferrocenemethanol have been reported as $D = 6.3 - 46 \cdot 10^{-12} \text{ m}^2 \text{ s}^{-1}$ in [EMIm][NTf₂] ($\eta = 34 \text{ mPa s}$)^{31,32} or $D = 25 \cdot 10^{-12} \text{ m}^2 \text{ s}^{-1}$ in [BMIm][NTf₂] and $D = 5 \cdot 10^{-12} \text{ m}^2 \text{ s}^{-1}$ in [BMIm][PF₆].^{30b} Lower diffusion coefficient values have been found for a rhenium tetrazolato complex^{18b} ($D = 5.8 \cdot 10^{-12} \text{ m}^2 \text{ s}^{-1}$ in [BMIm][NTf₂] and $D = 1.3 \cdot 10^{-12} \text{ m}^2 \text{ s}^{-1}$ in [BMIm][PF₆]) or for a large polyoxometalate ion^{18c} [Mo₆O₁₉]²⁻ ($D = 1.4 \cdot 10^{-12} \text{ m}^2 \text{ s}^{-1}$ in [BMIm][PF₆]).

Variation of the redox potentials of $[\text{Cu}^{\text{II}}(\text{TMPA})(\text{H}_2\text{O})]^{2+}$ vs the media.

As shown in Table 4, the value of the redox potential E_1^0 is highly dependent on the medium and on the amount of water present in that medium. Addition of water results in a large negative shift of the potential values except in CH_2Cl_2 . In this latter medium, the “dry” medium still contains a large amount of water regarding the water saturation value ($1.5 \cdot 10^{-1} \text{ mol L}^{-1}$) in CH_2Cl_2 , then the further addition of water does not lead to a considerable shift of the potential (20 mV). For the other media, a 120-140 mV shift of the apparent potential is observed. More surprising is the relative order of the apparent redox potential in the different media (Table 4). It varies according $E_1^0(\text{THF}) < E_1^0(\text{PC}) < E_1^0(\text{CH}_2\text{Cl}_2) < E_1^0([\text{BMIm}][\text{NTf}_2]) \leq E_1^0([\text{BMIm}][\text{PF}_6])$. As the polarity is increased (for instance THF to PC), the stabilization should be higher for the dication (Cu^{II}) than for the monocation (Cu^{I}). As a consequence, a negative shift of the redox potential is expected.³³ As shown in Table 4, the E_1^0 values varies with the media but not in the trend expected on the only basis of the dielectric constants values ($\text{PC} > [\text{BMIm}][\text{NTf}_2] \geq [\text{BMIm}][\text{PF}_6] > \text{CH}_2\text{Cl}_2 > \text{THF}$). Moreover, if we compare the “dry” THF medium with the “dry” ionic liquids media - because those media contain a similar amount of water- it can be observed that the apparent redox potential is positively shifted in the ionic liquids media ($\Delta E^0 = 60 \text{ mV}$). This effect is even stronger (140 mV) when the fifth ligand bound to Cu is a chloride ion (-0.75 V vs -0.61 V). Such a situation suggests that the Cu^{I} complex is better stabilized than the Cu^{II} cation. This observation can be related to specific solvation effect in ionic liquids media.³⁴ Ionic liquids are organised media and the Cu^{I} complex is likely to induce much less disorder than its corresponding Cu^{II} analogue, leading to an apparent stabilization of the cupric complex (entropic factor).

Medium effects on the kinetics of the reduction process of $[\text{Cu}^{\text{II}}(\text{TMPA})(\text{H}_2\text{O})]^{2+}$.

A further analyse of the electrochemical behaviour of the $[\text{Cu}^{\text{II}}(\text{TMPA})(\text{H}_2\text{O})]^{2+}$ complex allows to explore in more details the dynamics of the process namely regarding its kinetics. First, we will consider the apparent heterogeneous electron-transfer kinetics of the process in “dry” and “wet” media. One problem for measuring the associated rate constant with cyclic voltammetry is the large resistance resulting from low conductive media as those used in this work and which is somewhat difficult to mitigate with the positive feedback compensation feature included in most of the commercially available potentiostat. A way to overcome this difficulty is to use electrochemical impedance spectroscopy (EIS) that permits to determine the apparent heterogeneous electron-transfer kinetic rate constant from a charge transfer resistance (R_{ct}) measurement separated from the uncompensated solution resistance (R_{unc}). EIS was performed in the different media for dry and wet conditions.³⁵ As depicted in Fig. 6 for $[\text{BMIm}][\text{NTf}_2]$, the addition of water systematically leads to a variation of the Nyquist Plots (Z'' vs Z' where Z'' and Z' correspond to the imaginary and real part of the impedance respectively). Reasonable fits of the experimental

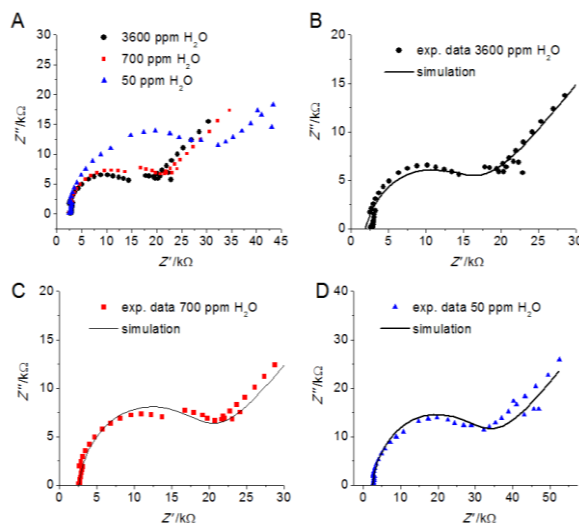
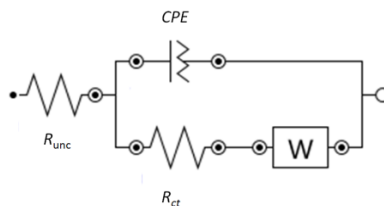


Fig. 6. Nyquist plots (Z'' vs Z') from EIS measurements at a glassy carbon electrode of $[\text{Cu}^{\text{II}}(\text{TMPA})(\text{H}_2\text{O})]^{2+}$ in $[\text{BMIm}][\text{NTf}_2]$ upon addition of water ($E_{\text{ac}} = 0.01 \text{ V}$, $0.1 \text{ Hz} < \omega < 10^4 \text{ Hz}$). A) $[\text{H}_2\text{O}] = 4 \cdot 10^{-3} \text{ mol L}^{-1}$ (50 ppm) (\blacktriangle), $[\text{H}_2\text{O}] = 6 \cdot 10^{-2} \text{ mol L}^{-1}$ (700 ppm) (\blacksquare), and $[\text{H}_2\text{O}] = 2.9 \cdot 10^{-1} \text{ mol L}^{-1}$ (3600 ppm) (\bullet); B) $[\text{H}_2\text{O}] = 2.9 \cdot 10^{-1} \text{ mol L}^{-1}$ (3600 ppm) exp. data and simulated curve on the basis of the equivalent circuit in Scheme 1; C) $[\text{H}_2\text{O}] = 6 \cdot 10^{-2} \text{ mol L}^{-1}$ (700 ppm) exp. data and simulated curve; D) $[\text{H}_2\text{O}] = 4 \cdot 10^{-3} \text{ mol L}^{-1}$ (50 ppm) exp. data and simulated curve.

curves were obtained on the basis of a classical equivalent circuit modelling the electrochemical cell including a constant phase element (CPE) (instead of a pure double layer capacitance) and a Warburg impedance (W) (related to the diffusion limiting process) (Scheme 2). The Nyquist plots fitting provides a determination of R_{ct} values then of the apparent electron transfer rate constant k_{app} in the different media, under “dry” and “wet” conditions. Results are gathered in Table 5 for comparison purpose. For any of the media used in this work, the overall electrochemical process appears as a very slow process since the reported k_{app} values are small. The addition of water results in an enhancement of the apparent electron-transfer kinetics, indicating that the overall kinetics depends on the water concentration in the medium. This suggests that the reduction process of the $[\text{Cu}^{\text{II}}(\text{TMPA})(\text{H}_2\text{O})]^{2+}$ complex involves chemical

reactions (H₂O coordination/decoordination) that are faster than the electrochemical reaction as previously described by Laviron in a square scheme mechanism.^{35,36}



Scheme 2. Equivalent circuit used for experimental impedance simulation. R_{unc} : uncompensated solution resistance; R_{ct} : charge transfer resistance; CPE: constant-phase element; W: Warburg impedance.

Table 5 Apparent heterogeneous electron-transfer kinetic rate constant ($k_{app}/\text{cm s}^{-1}$) values in different media (dry/wet) from Nyquist plots fitting.

	“dry” medium		“wet” medium	
	[H ₂ O]/ mol L ⁻¹	$k_{app}/$ cm s ⁻¹	[H ₂ O]/ mol L ⁻¹	$k_{app}/$ cm s ⁻¹
CH ₂ Cl ₂	1.5 10 ⁻²	1.4 10 ⁻⁴	1.4 10 ⁻¹	7.1 10 ⁻⁴
THF	2.5 10 ⁻³	2.3 10 ⁻⁴	9.4 10 ⁻²	4.1 10 ⁻⁴
PC	9.9 10 ⁻³	2.3 10 ⁻⁴	4.5 10 ⁻¹	6.7 10 ⁻⁴
[BMIm][NTf ₂]	4 10 ⁻³	5 10 ⁻⁵	2.9 10 ⁻¹	9 10 ⁻⁵
[BMIm][PF ₆]	5.8 10 ⁻³	1 10 ⁻⁵	2.0 10 ⁻¹	8 10 ⁻⁵

The comparison of k_{app} values between organic solvents and the ionic liquids clearly shows (for both dry and wet conditions) a slower electron transfer process in the IL media. This effect was already reported for different electroactive species.^{31,37} From a kinetic point of view, IL could affect the activation energy, through solvent-solute interactions, dynamic solvent effects, as well as the entropic term because of the strong structuration of the media. In the framework of the Marcus-Hush theory, outer-sphere electron transfer kinetics could be expressed under its Arrhenius form (equation (2)):

$$k_{app} = \kappa K_p \tau_L^{-1} \left[\frac{-\Delta G^*}{4\pi RT} \right]^{1/2} \exp \left[\frac{-\Delta G^*}{RT} \right] \quad (2)$$

where κ is the probability of electron tunnelling (1 in case of adiabicity), K_p is the equilibrium constant for a precursor model, τ_L is the longitudinal relaxation time, ΔG^* is the activation energy.

A recent theoretical work on the use of Marcus theory to redox processes in RTILs has predicted that lower rate constants obtained in ionic liquid vs usual organic solvents could be due to solvent dynamics, i.e the τ_L parameter from the pre-exponential factor in equation (2).³⁸ Indeed, screening times are supposed to be higher in ionic liquids than in organic solvents. It has been suggested that this could result from slow translational motion of the ions in the ionic liquid media whereas fast longitudinal relaxation occur in organic solvents.

Voltammetric simulations

The cyclic voltammetry experiments as described in Fig. 3 are in agreement with an electron transfer associated with a slow (at the cyclic voltammetry timescale) decoordination of the H₂O axial ligand when Cu^{II} is reduced to Cu^I. The anodic peak located at *ca.* 0.4 V vs Fc is H₂O-related and arises upon the reduction of Cu^{II} complex to Cu^I complex. This irreversible oxidation peak could be reasonably ascribed to the cuprous complex with no water molecule bounded to Cu^I. This is supported by the fact that the oxidation potential corresponding to the formed [Cu^I(TMPA)]⁺ is hardly affected by the media since a value $E_p \sim 0.4$ V vs Fc is found in all the four media. Notice that this system remains totally irreversible for all the scan rates, up to 20 V s⁻¹, and its oxidation occurs at a potential around 0.7 V more positive than the aqua complex. We could derive that, contrarily to [Cu^I(TMPA)]⁺, the binding of water to [Cu^{II}(TMPA)]²⁺ is fast and totally irreversible.

Scheme 3. Formal square scheme mechanism for the exchange of water associated with electron transfer for the $[\text{Cu}^{\text{II}}(\text{TMPA})(\text{H}_2\text{O})]^{2+}$ complex.

The electrochemical process can be then described as in scheme3: $[\text{Cu}^{\text{II}}(\text{TMPA})(\text{H}_2\text{O})]^{2+}$ is first reduced to $[\text{Cu}^{\text{I}}(\text{TMPA})(\text{H}_2\text{O})]^+$ and a slow decoordination of the H_2O axial ligand is following to produce a cuprous complex $[\text{Cu}^{\text{I}}(\text{TMPA})]^+$ which is oxidized on the return scan. The 4-coordinate Cu species likely displays a pseudo-tetrahedral environment in agreement with previous studies.^{39,40} Voltammograms of Fig. 3 and 4 were simulated (see Fig. S1) to extract the kinetic (k_b , k_f) and thermodynamic ($K = k_b/k_f$) parameters associated to the binding/unbinding at the Cu^{I} redox state according to Scheme 3.⁴¹ It was possible to get a good agreement between experimental and fitted parameters considering the mechanism depicted in Scheme 3. Two criteria could be considered to extract the data. The reversibility of the reduction of $[\text{Cu}^{\text{II}}(\text{TMPA})(\text{H}_2\text{O})]^{2+}$ considerably increases with the scan rates from 0.02 to 0.5 V s^{-1} . Similarly, the reversibility increases with an addition of water in the media. These two observations imply that the reaction of $[\text{Cu}^{\text{I}}(\text{TMPA})]^+$ with H_2O is relatively slow and equilibrated.

Table 6 Kinetics and thermodynamic parameters of the dissociation reaction of $[\text{Cu}^{\text{I}}(\text{TMPA})(\text{H}_2\text{O})]^+$ [a]

Medium	k_f / s^{-1}	$k_b / \text{L mol}^{-1} \text{s}^{-1}$	$K / \text{L mol}^{-1}$
THF	0.15	4	26
PC	0.02	4	200
[BmIm][NTf ₂]	0.08	20	250

[a] Estimations from simulations of experimental voltammograms (See Fig. S1 and Supplementary Information part).

These conclusions are illustrated by the derived rate constants of Table 6. On the whole, there is little change with the solvent. We just notice that the H_2O binding is more favoured and faster in the ionic liquid than in the two other classical solvents. On one hand, the sluggishness of the decoordination process in all media may be associated to the fact that pyridyl moities can be very labile at Cu^{I} redox state when an exogenous ligand is bounded, as previously reported.^{39,42} Indeed, the pyridyl decoordination may induce a reinforcement of the metal-water bond, thus disfavoring water departure. On the other hand, the higher kinetics for the water binding reaction at Cu^{I} detected for the imidazolium-based ionic liquids vs THF and PC may be ascribed to the existence of specific domains in these media which significantly favour the diffusion of water molecules despite high viscosity.⁴³ This behaviour is reminiscent of channel enzymes⁴⁴ and could be exploited in catalytic reactions involving fast water coordination/decoordination.

Conclusions

The coordination behaviour of a mononuclear complex $[\text{Cu}^{\text{II}}(\text{TMPA})(\text{H}_2\text{O})]^{2+}$, simple mimic of metallo enzymes was investigated in different non-coordinating solvents, including IL, by combining electrochemistry and spectroscopic techniques. Only a few studies report on the fundamental behaviour of inorganic metal complexes in IL. The coordination geometry of the Cu^{II} complex remains trigonal bipyramidal in all the media with the water ligand being axially coordinated to Cu^{II} . In particular, the anions of the ionic liquids were not found to coordinate the copper centre. The dissociation mechanism of the water axial ligand upon electron transfer in terms of kinetics and thermodynamics was studied in different media. The overall process is highly dependent on the water concentration, with a slow electron transfer reaction, slower in ionic liquids than in the conventional solvents, as already reported for different electroactive species. The decoordination of the water molecule was detected by cyclic voltammetry from the monoelectronic reduction of the Cu^{II} complex. The increase of the water content and/or decrease of the timescale of the experiment resulted in the disappearance of the oxidation peak related to the water-free Cu^{I} complex. Numerical simulations of the experimental CVs suggest that the binding/unbinding of water at the Cu^{I} redox state is relatively slow and equilibrated in all media. Moreover, the binding of water at Cu^{I} is somewhat faster in the ionic liquids than in the non-coordinating conventional solvents, while the unbinding process is weakly

sensitive to the nature of the solvents.

In summary, the ionic liquids exhibit promising properties in comparison to classical solvents, to investigate redox systems which are Cu-enzymes models: (i) no coordination of the anion to the metal ion at any redox state, (ii) enhanced water flow/exchange, and (iii) tunable molecular structure (shape and bulkyness). This last property can be exploited for investigating host-guest reactions with biomimetic systems incorporating cavities such as calix[6]arene,^{1b-c,10} since adequate design of the RTILs can preclude competitive solvent hosting and thus promote better access of the substrate to the cavity.

Experimental

Materials and methods

10 Anhydrous “extra-dry” dichloromethane ($H_2O < 30$ ppm, Acros), tetrahydrofuran (99.85%, Acros), and propylene carbonate (99.7%, Sigma-Aldrich) were used as received and kept under N_2 in the glovebox. CH_2Cl_2 , THF and PC were dried on activated molecular sieves in the glovebox before use. All chemicals were of reagent grade and were used without purification. The supporting electrolyte NBu_4PF_6 was synthesized from NBu_4OH (Fluka) and HPF_6 (Aldrich). It was then purified, dried under vacuum for 48 hours at $100^\circ C$, then kept under N_2 in the glovebox. EPR spectra were run at $T=150$ K on a Bruker Elexsys spectrometer (X-band). EPR simulation was carried
15 on the XSophe-Sophe-Xpreview software and afforded the quantitative determination of the g_{\perp} and g_{\parallel} parameters as well as the related hyperfine coupling constants A_{\perp} and A_{\parallel} .⁴⁵ UV-Vis-NIR spectroscopy was performed with a JASCO V-670 spectrophotometer and an integration-sphere accessory for solid-state measurements. The electrochemical studies were performed in a glovebox (Jacomex) ($O_2 < 1$ ppm, $H_2O < 1$ ppm) with a home-designed 3-electrodes cell (Working electrode: glassy carbon disk, reference electrode: Pt in Fc^+/Fc solution, counter electrode: Pt wire). The glassy carbon electrode was carefully polished before each voltammetry experiment
20 with a $3 \mu m$ alumina aqueous suspension and ultrasonically rinsed in water then acetone. The concentration in Cu complex was $10^{-3} mol L^{-1}$ except in the ionic liquid where the concentration was set to $3 \cdot 10^{-3} mol \cdot L^{-1}$, in order to get a better signal-to-noise ratio. All potential values are given against the ferrocene/ferrocenium couple. Cyclic voltammetry and impedance spectroscopy measurements were performed with an Autolab electrochemical analyzer (PGSTAT 302 potentiostat/galvanostat from Eco Chemie B.V., equipped with the GPES/FRA software). For cyclic voltammetry, scan rates were varied between 0.02 and $5 V s^{-1}$. For impedance spectroscopy, a 10
25 mV rms sinusoidal signal was applied along with the dc potential, which was set at the E^0 value previously determined by cyclic voltammetry. The frequency range was varied from 0.1 Hz to 10 kHz. The charge transfer resistance value (R_{ct}) was extracted from the experimental Nyquist plots on the basis of the equivalent circuit. The apparent rate constant k_{app} was evaluated from the simplification of the Butler-Volmer equation at small overpotential (equation (3)), assuming that $\alpha = 0.5$ and $C_O = C_R$ at the equilibrium potential.

[R is the perfect gas constant, T is the absolute temperature, n the number of electrons exchanges, F the Faraday constant, A is the
30 electrode area, C_O and C_R are the bulk concentrations of the oxidized and reduced species, α is the symmetry barrier coefficient and was taken as 0.5].

$$R_{ct} = \frac{RT}{n^2 F^2 A k_{app} C_O^{(1-\alpha)} C_R^{\alpha}} \quad (3)$$

Synthesis of the ligand and Cu complex

The TMPA ligand (TMPA = tris(2-pyridylmethyl)amine) was prepared according to a previously published procedure.⁴⁶

The synthesis of the bis-triflate Cu complex $[Cu^{II}(TMPA)(H_2O)](CF_3SO_3)_2$ was operated by addition of equimolar amounts of $Cu^{II}(CF_3SO_3)_2$ to a solution of the TMPA ligand (toluene), leading to the formation of a blue powder. After evaporation of the solvent
40 and washing with diethyl ether, the compound was dissolved in THF. Slow evaporation of the solvent afforded blue crystals identified by X-ray diffraction analysis as the mono-aqua copper (II) complex, $[Cu^{II}(TMPA)(H_2O)](CF_3SO_3)_2$.

Synthesis of the ionic liquids

The room temperature ionic liquids $[BMIm][NTf_2]$, $[BMIm][PF_6]$ and $[Et_3BuN][NTf_2]$ were prepared according to standard procedures⁴⁷
45 from mixing aqueous $LiNTf_2$ (Sigma-Aldrich or Solvionic) or $NaPF_6$ (Sigma-Aldrich), and aqueous $BMImCl$ (Sigma-Aldrich or Solvionic) or Et_3BuNCl . The samples were purified by repeated washing with H_2O , filtered over neutral alumina and silica. Prior to each experiment, vacuum pumping carefully dried RTIL overnight and then dried over molecular sieves at least for 48 h. The amount of water was measured by Karl Fischer titration (Karl Fischer 652 Metrohm).

Acknowledgments

This research was supported by CNRS, Ministère de la Recherche et de l'Enseignement Supérieur (A. G.), Conseil Régional de Bretagne (J. Z.) and Agence Nationale pour la Recherche (ANR-2010-BLAN-0714, Cavity-zyme (Cu)). Dr F. Michaud is thanked for XRD analyses and Mohammad Kassem for the synthesis of the Cu^{II} complex from tmpa ligand.

Notes and references

^a Laboratoire de Chimie, Electrochimie Moléculaires et Chimie Analytique, CNRS, UMR 6521, Université de Brest, 6 av. Le Gorgeu, 29328 Brest cedex, France; Fax: +33298017001; Tel: +33298016168; E-mail: nicolas.lepoul@univ-brest.fr

^b Laboratoire de Chimie et Biochimie Pharmacologiques et Toxicologiques, CNRS, UMR 8601, Université Paris Descartes, 45 rue des Saints-Pères, 75006 Paris, France.

¹⁰ ^c Institut des Sciences Chimiques de Rennes, Equipe MacCSE, CNRS, UMR 6226, Université de Rennes 1, Campus de Beaulieu, 35042 Rennes, France ; Fax: +33223236732; Tel: +33223235940; E-mail : corinne.lagrost@univ-rennes1.fr.

† Electronic Supplementary Information (ESI) available: numerical simulations of cyclic voltammetry experiments and XRD data collection (CCDC 946244). See DOI: 10.1039/b000000x/.

‡ Addition of chloride ions leads to the increase of the intensity of the redox system at -0.61 V vs Fc/Fc⁺.

¹⁵ #The E_{dc} potential was systematically determined from the cyclic voltammetric curve before ac impedance measurement by taking the mid-potential value for different water concentrations.

- 1 [a] D. B. Rorabacher, *Chem. Rev.*, 2004, **104**, 651; [b] N. Le Poul, M. Campion, G. Izzet, B. Douziech, O. Reinaud and Y. Le Mest, *J. Am. Chem. Soc.*, 2005, **127**, 5280; [c] N. Le Poul, M. Campion, B. Douziech, Y. Rondelez, L. Le Clainche, O. Reinaud, Y. Le Mest, *J. Am. Chem. Soc.*, 2007, **129**, 8801.
- 2 [a] K. D. Karlin, J. C. Hayes, S. Juen, J. P. Hutchinson and J. Zubieta, *Inorg. Chem.*, 1982, **21**, 4106; [b] P. L. Dedert, Thompson, J. S., J. A. Ibers and T. J. Marks, *Inorg. Chem.*, 1982, **21**, 969.
- 3 [a] L. M. Mirica, X. Ottenwaelde and T. D. P. Stack, *Chem. Rev.*, 2004, **104**, 1013; [b] E. A. Lewis and W. B. Tolman, *Chem. Rev.*, 2004, **104**, 1047.
- 4 A. G. Blackman, *Eur. J. Inorg. Chem.*, 2008, 2633.
- 5 K. D. Karlin, S. Itoh, Copper-Oxygen Chemistry, John Wiley & Sons, Inc., Hoboken, New Jersey, 2011.
- 6 Y. Tachi, Y. Matsukawa, J. Teraoka and S. Itoh, *Chem. Lett.*, 2009, **38**, 202-203.
- 7 [a] H. R. Lucas, L. Li, A. A. N. Sarjeant, M. A. Vance, E. I. Solomon and K. D. Karlin, *J. Am. Chem. Soc.*, 2009, **131**, 3230; [b] C. Würtele, O. Sander, V. Lutz, T. Waitz, F. Tuczek and S. Schindler, *J. Am. Chem. Soc.*, 2009, **131**, 7544.
- 8 M. A. Thorseth, C. S. Letko, T. B. Rauchfuss and A. A. Gewirth, *Inorg. Chem.*, 2011, **133**, 3696.
- 9 H. Nagao, N. Komeda, M. Mukaida, M. Suzuki and K. Tanaka, *Inorg. Chem.*, 1996, **35**, 6809.
- 10 N. Le Poul, B. Douziech, J. Zeitouny, G. Thiabaud, H. Colas, F. Conan, N. Cosquer, I. Jabin, C. Lagrost, P. Hapiot, O. Reinaud and Y. Le Mest, *J. Am. Chem. Soc.*, 2009, **131**, 17800.
- 11 P. Ball, *Chem. Rev.*, 2008, **108**, 74.
- 12 J. P. Collman R. A. Decreau, A. Dey, Y. Yang, *Proc. Natl. Acad. Sci. USA*, 2009, **106**, 4101.
- 13 A. Dey, F. E. Jenney Jr., M. W. W. Adams, E. Babini, Y. Takahashi, K. Fukuyama, K. O. Hodgson, B. Hedman, E. I. Solomon, *Science*, 2007, **318**, 1464.
- 14 S. V. Antonyuk, C. Han, R. R. Eady, S. S. Hasnain, *Nature*, 2013, **496**, 123.
- 15 [a] T. Welton, *Chem. Rev.*, 1999, **99**, 2071; [b] P. Wasserscheid and T. Welton, *Ionic Liquids in Synthesis*, 2003, Wiley-VCH, Weinheim, Germany; [c] R. D. Rogers and K. R. Seddon, in 'Ionic Liquids IIIB: Fundamentals, Progress, Challenges, and Opportunities: Transformations and Processes, ACS Symposium Series 902', Washington, DC, 2005.
- 16 [a] S. Pandey *Anal. Chim. Acta*, 2006, **556**, 38; [b] J. Liu, J. A. Jönsson and G. Jiang, *Trends Anal. Chem.*, 2005, **24**, 20; [c] W. Wei and A. Ivaska, *Anal. Chim. Acta*, 2008, **607**, 126; [d] D. V. Chernyshov, N. V. Shvedene, E. R. Antipova and I. V. Pletnev, *Anal. Chim. Acta*, 2008, **621**, 178; [e] H. Olivier-Bourbigou, L. Magna and D. Mován, *Appl. Catal. A: Gen.*, 2010, **373**, 1; [f] K. Fujita, K. Murata, M. Masuda, N. Nakamura and H. Ohno, *RSC Adv.*, 2012, **2**, 4018; [g] D. S. Silvester, *Analyst*, 2011, **136**, 4871; [h] F. Endres and S. Z. El Abedin, *Phys. Chem. Chem. Phys.*, 2006, **8**, 2101; [i] M. Armand, F. Endres, D. R. MacFarlane, H. Ohno and B. Scrosati, *Nature Mat.*, 2009, **8**, 621.
- 17 [a] P. Hapiot and C. Lagrost, *Chem. Rev.*, 2008, **108**, 2238; [b] D. S. Silvester and R. G. Compton, *Z. Phys. Chem.*, 2006, **220**, 1247; [c] M. C. Buzzeo, R. G. Evans and R. G. Compton, *ChemPhysChem*, 2006, **5**, 1106.
- 18 [a] Y. Pan and C. L. Hussey, *Inorg. Chem.*, 2013, **52**, 3241; [b] D. S. Silvester, S. Uprety, P. J. Wright, M. Massi, S. Stagni and S. Muzzioli, *J. Phys. Chem. C*, 2012, **116**, 7327; [c] J. Zhang, A. M. Bond, D. R. MacFarlane, S. A. Forsyth, J. M. Pringle, A. W. A. Mariotti, A. F. Glowinski and A. G. Wedd, *Inorg. Chem.*, 2005, **44**, 5123; [d] S. I. Nikitenko and P. Moisy, *Inorg. Chem.*, 2006, **45**, 1235; [e] M. Deetlefs, C. L. Hussey, T. J. Mohammed, K. R. Seddon, J.-A. van den Berg and J. A. Zora, *Dalton Trans.*, 2006, 2234.

- 19 [a] P. Illner, R. Puchta, F. W. Heinemann and R. van Eldik, *Dalton Trans.*, 2009, 2795; [b] M. Schmeisser, F. W. Heinemann, P. Illner, R. Puchta, A. Zahl and R. van Eldik, *Inorg. Chem.*, 2011, **50**, 6685.
- 20 S. Caporali, C. Chiappe, T. Ghilardi, C. S. Pomelli and C. Pinzino, *ChemPhysChem*, 2012, **13**, 1885.
- 21 A. W. Addison, T. N. Rao, J. Reedijk, J. van Rijn and G. C. Verschoor, *J. Chem. Soc., Dalton Trans.*, 1984, 1349.
- 22 D. B. Williams, M. E. Stoll, B. L. Scott, D. A. Costa and W. J. Oldham Jr, *Chem. Commun.*, 2005, 1438.
- 23 B. J. Hathaway and D. E. Billing, *Coord. Chem. Rev.*, 1970, **5**, 143.
- 24 [a] C. Dagueuet, P. J. Dyson, I. Krossing, A. Oleinikova, J. Slattery, C. Wakai and H. Weingärtner, *J. Phys. Chem. B*, 2006, **110**, 12682; [b] C. Wakai, A. Oleinikova, M. Ott and H. Weingärtner, *J. Phys. Chem. B*, 2005, **109**, 17028.
- 25 [a] D. R. Lide, (ed.) *CRC Handbook of Chemistry and Physics*, 85th Ed.; CRC Press: Boca Raton, FL (USA), 2004-2005; [b] P. Bonhôte, A.-P. Dias, N. Papageorgiou, K. Kalyanasundaram and M. Grätzel, *Inorg. Chem.*, 1996, **35**, 1168.
- 26 R. R. Jacobson, Z. Tyeklar and K. D. Karlin, *Inorg. Chim. Acta*, 1991, **181**, 111.
- 27 A. J. Bard and L. R. Faulkner, *Electrochemical methods*, Wiley and sons, New York, 2001.
- 28 [a] D. S. Silvester, K. L. Ward, L. Aldous, C. Hardacre and R. G. Compton, *J. Electroanal. Chem.*, 2008, **618**, 53; [b] L. E. Barrosse-Antle, D. S. Silvester, L. Aldous, C. Hardacre and R. G. Compton, *J. Phys. Chem. C*, 2008, **112**, 2729.
- 29 [a] M. Zistler, P. Wachter, P. Wasserscheid, D. Gerhard, A. Hinsch, R. Sastrawan and H. J. Gores, *Electrochimica Acta*, 2006, **160**, 125; [b] R. Kawano and M. Watanabe, *Chem. Commun.*, 2005, 2107.
- 30 [a] A. W. Taylor, P. Licence and A. P. Abbott, *Phys. Chem. Chem. Phys.*, 2011, **13**, 10147; [b] K. R. J. Lovelock, A. Ejigu, S. F. Loh, S. Men, P. Licence and D. A. Walsh, *Phys. Chem. Chem. Phys.*, 2011, **13**, 10155.
- 31 C. Lagrost, D. Carrié, M. Vaultier and P. Hapiot, *J. Phys. Chem. A*, 2003, **107**, 745.
- 32 A. S. Barnes, E. I. Rogers, I. Streeter, L. Aldous, C. Hardacre and R. G. Compton, *J. Phys. Chem. B*, 2008, **112**, 7560.
- 33 P. Zanello, *Inorganic Electrochemistry, theory, practice and application*, The Royal Society of Chemistry, Cambridge, 2003.
- 34 [a] A. A. H. Pádua, M. F. Costa Gomes and J. N. A. Canongia Lopes, *Acc. Chem. Res.*, 2007, **40**, 1087; [b] J. N. Canongia Lopes, M. F. Costa Gomes, P. Husson, A. A. H. Pádua, L. P. N. Rebelo, S. Sarraute and M. Tariq, *J. Phys. Chem. B*, 2011, **115**, 6088.
- 35 E. Laviron and L. Roullier, *J. Electroanal. Chem.*, 1985, **186**, 1.
- 36 E. Laviron, *J. Electroanal. Chem.*, 1980, **109**, 57.
- 37 [a] C. Lagrost, L. Preda, E. Volanschi and P. Hapiot, *J. Electroanal. Chem.*, 2005, **585**, 1; [b] N. Fietkau, A. D. Clegg, R. G. Evans, C. Villagran, C. Hardacre and R. Compton, *ChemPhysChem*, 2006, **7**, 1041.
- 38 R. M. Lynden-Bell, *Electrochem. Commun.*, 2007, **9**, 1857.
- 39 D.-H. Lee, N. Wei, N. N. Murthy, Z. Tyeklar, K. D. Karlin, S. Kaderli, B. Jung, A. D. Zuberbühler, *J. Am. Chem. Soc.*, 1995, **117**, 12498.
- 40 [a] H. R. Lucas, G. J. Meyer, K. D. Karlin, *J. Am. Chem. Soc.*, 2010, **132**, 12927; [b] H. C. Fry, H. R. Lucas, A. A. Narducci Sarjeant, K. D. Karlin, G. J. Meyer, *Inorg. Chem.* 2008, **47**, 241; [c] Z. Tyeklar, R. R. Jacobson, N. Wei, N. Narasimha Murthy, J. Zubietta, K. D. Karlin, *J. Am. Chem. Soc.*, 1993, **115**, 2677; [d] B. S. Lim, R. H. Holm, *Inorg. Chem.*, 1998, **37**, 4898.
- 41 [a] Kissa 1D Software package; [b] C. Amatore, O. Klymenko and I. Svir *Electrochem. Commun.*, 2010, **12**, 1165; [c] C. Amatore, O. Klymenko and I. Svir, *Electrochem. Commun.*, 2010, **12**, 1170.
- 42 L. Bonniard, A. de la Lande, S. Ulmer, J. P. Piquemal, O. Parisel and H. Gerard, *Catal. Tod*, 2011, **177**, 79.
- 43 A.-L. Rollet, P. Porion, M. Vaultier, I. Billard, M. Deschamps, C. Bessada, and L. Jouvensal, *J. Phys. Chem. B*, 2007, **111**, 11888;
- 44 [a] H.-X. Zhou and J. A. McCammon, *Trends Biochem Sci.*, 2010, **35**, 179; [b] A. Gora, J. Brezovsky, J. Damborsky, *Chem. Rev.*, 2013, **113**, 5871.
- 45 G. R. Hanson, K. E. Gates, C. J. Noble, M. Griffin, A. Mitchell and S. Benson, *J. Inorg. Biochem.*, 2004, **98**, 903.
- 46 Z. Tyeklár, R. R. Jacobson, N. Wei, N. N. Murthy, J. Zubietta and K. D. Karlin, *J. Am. Chem. Soc.*, 1993, **115**, 2677.
- 47 P. Bonhôte, A. P. Dias, N. Papageorgiou, K. Kalyanasundaram and M. Grätzel, *Inorg. Chem.*, 1996, **35**, 1168.